Earth and Planetary Science Letters 304 (2011) 64–70

Contents lists available at ScienceDirect

Earth and Planetary Science Letters

journal homepage: www.elsevier.com/locate/epsl

Monitoring aseismic surface creep along the North Anatolian Fault (Turkey) using ground-based LIDAR

V. Karabacak [a,*], E. Altunel [a], Z. Cakir [b]

[a] Eskisehir Osmangazi University, Department of Geological Engineering, 26480, Eskisehir, Turkey
[b] Istanbul Technical University, Department of Geological Engineering, 34469, İstanbul, Turkey

ARTICLE INFO

Article history:
Received 13 July 2010
Received in revised form 17 January 2011
Accepted 18 January 2011
Available online 20 February 2011

Editor: T.M. Harrison

Keywords:
North Anatolian Fault
creep
aseismic surface slip
light detection and ranging (LIDAR)

ABSTRACT

We studied the surface creep along the North Anatolian Fault (NAF), one of the most seismically active structures of the eastern Mediterranean, by using a ground-based light detection and ranging (LIDAR) system at the Ismetpasa and Destek sections. Aseismic surface creep has been known to exist at Ismetpasa since the 1970s, but it has not been previously reported for the Destek site. Three manmade walls across the fault were monitored for 3 yrs between June 2007 and November 2009 using LIDAR. The surveys revealed that a significant amount of aseismic strain is being continuously released along these sections of the NAF: 6.8–10.0 ± 4.0 mm/yr and 9.1–10.1 ± 4.0 mm/yr at two sites near Ismetpasa and 6.0–7.2 ± 4.0 mm/yr at Destek. Despite this, these fault segments are still capable of generating large earthquakes since 50–70% of the yearly slip (i.e., 20–25 mm/yr) still accumulates on the fault, as was demonstrated by the well-known 20th century earthquake sequence of 1939–1999.

1. Introduction

The sudden release of accumulated strain on locked active faults produces large and destructive earthquakes. However, the strain on some faults is partially or even entirely unloaded without the occurrence of earthquakes. If the rate of aseismic slip is equal to or larger than the long-term slip rate, large earthquakes will not be generated (such as in the case of the central San Andreas Fault; Burtford and Harsh, 1980; Thatcher, 1979). On the other hand, if the creep motion is much lower than the long-term slip rate along a fault, then the fault is still capable of producing moderate-to-large size earthquakes (such as in the case of the southern and northern Hayward Fault; Lienkaemper and Williams, 1999; Schimdt et al., 2005). Therefore, it is important to understand the behaviour of active faults to evaluate the seismic hazard of the surrounding regions.

The North Anatolian Fault (NAF) is one of the most seismically active structures in the world. Constraints on the slip rates along the NAF have been obtained from the Global Positioning System (GPS) as well as from geomorphic and geologic observations. For example, dextral strike-slip rates of approximately 18–20 mm/yr have been estimated by using offset features over the last 2–3 ka (Kozacı et al., 2007, 2009) and 10–12 ka (Hubert-Ferrari et al., 2002) time periods. Block models constrained by GPS data indicate dextral strike-slip rates of 22–26 mm/yr along the NAF (e.g. McClusky et al., 2000; Reilinger et al., 2006). At this slip rate, strain accumulates over a long period of time, and several large earthquakes have occurred as a result (e.g. 1943 Tosya [Ms = 7.6], 1944 Bolu-Gerede [Ms = 7.3], 1999 Izmit [Ms = 7.4], and 1999 Duzce [Ms = 7.2], Fig. 1a). However, some sections of the NAF are known to exhibit aseismic slip at the Earth's surface (Cakir et al., 2005). Therefore, the monitoring of the creep and comparing the results with the long-term slip rate are essential for evaluating the earthquake hazard along these NAF segments.

Aseismic surface slip has long been known to be taking place on the NAF near Ismetpasa in northwest Turkey (Ambraseys, 1970). Various techniques have been used to deduce the creep rate on this section. Ambraseys (1970) estimated a creep rate of about 20 mm/yr for the period between 1957 and 1969 by measuring the offset on the warped wall of a railway station, where the phenomenon of surface creep was discovered. Measurements on a creepmeter installed nearby and the local triangulation network several kilometres to the east provided creep rates of about 7–12 mm/yr until the 1990s (Altay and Sav, 1991; Aytun, 1982; Deniz et al., 1993). Cakir et al. (2005) estimated a creep rate of 8 ± 3 mm/yr around the railway station by using synthetic aperture radar interferometry (InSAR). Kutoglu and Akcın (2006) surveyed the same geodetic network using GPS and estimated a creep rate of 7.8 ± 0.5 mm/yr. These measurements clearly show that the creep rate decreased with time. More recently, however, Kutoglu et al. (2008) reported a sudden increase in the creep rate reaching 12 ± 1.1 mm/yr between 2002 and 2007. However, it is not clear whether the creep rate is now increasing for some unknown reasons or whether it was somehow overestimated by Kutoglu et al. (2008). Thus, new measurements must be obtained to

* Corresponding author at: Eskisehir Osmangazi University, Department of Geology, 26040, Eskisehir, Turkey. Tel.: +90 222 2393750/3408; fax: +90 222 2290535.
E-mail address: karabacak@ogu.edu.tr (V. Karabacak).

0012-821X/$ – see front matter © 2011 Elsevier B.V. All rights reserved.
doi:10.1016/j.epsl.2011.01.017

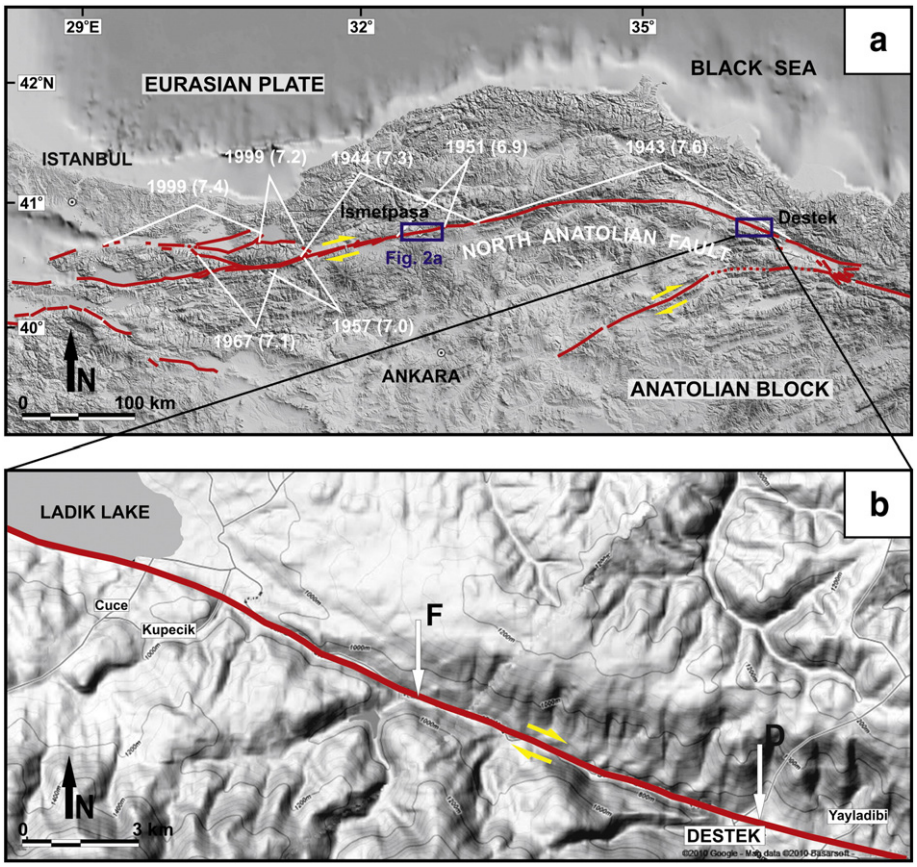

Fig. 1. (a) Simplified map of the North Anatolian Fault showing creep locations and recent major earthquakes. (b) General trend of the North Anatolian Fault around Destek. "D" indicates the location of the surveyed area in Destek (Fig. 2b), and "F" shows the location of the paleoseismic trench performed by Fraser et al. (2009). Relief image is from Google Map software.

confirm the change in the creep rate. These measurements can also potentially provide insights for understanding the nature of the aseismic slip at Ismetpasa and elsewhere.

In this study, therefore, we decided to measure the surface creep rate at Ismetpasa. For this, we used LIDAR technology because it can provide high resolution and accurate 3D measurements in a very short time. This paper also discusses another creeping site along the 1943 Tosya earthquake rupture of the NAF (Fig. 1a and b), which was discovered by us during a reconnaissance survey carried out in 2003. Three walls across the fault line at these two sites were periodically scanned using LIDAR for 3 yrs. We present the results of these LIDAR surveys here and discuss the nature of the surface creep along the NAF.

2. Methodology

Ground-based LIDAR technology is an active remote sensing system and a new alternative to conventional geodetic techniques. This technology is based on measuring the travel time of a laser beam from the source to a target (Kemeny and Turner, 2008; Optech, 2006). Multiple laser beams sweeping the laser range allow the creation of a three-dimensional (3D) point cloud of the target surface at a millimetre-scale resolution. These point clouds are then commonly converted into triangulated surfaces and used for draping high-resolution digital photographs to create virtual-reality models of the surface (POB, 2008). Ground-based LIDAR technology is becoming more and more widely used across a range of earth science disciplines that require sensitive surveying of physiographic features (Bawden et al., 2004; Bellian et al., 2005; Bonnaffe et al., 2007; Ekercin and Üstün, 2004; Janson et al., 2007; Kayen, 2004; Kemeny and Turner, 2008; Nagihara, 2006; Niemi et al., 2004).

LIDAR is accurate to about 3 mm for a distance of 100 m according to the manufacturers (Kemeny and Turner, 2008; Optech, 2006; POB, 2008; Staiger, 2003). In addition, the field conditions and personnel capability contribute to the overall accuracy of the scanners in operations. For example, the overall accuracy is known to be affected by the distance and aspect angle to the targets (Kemeny and Turner, 2008; Optech, 2006; POB, 2008). At the beginning of this study, in consideration of the accuracy of ground-based LIDAR, two different targets were scanned from three different distances at medium (5 mm) and fine resolution (3 mm) settings in daylight (Supplementary Fig. S1). The obtained point clouds of each resolution and distance showed that the range accuracy of the LIDAR system changed between 2.7 and 5.2 mm (Table 1). Thus, this technology can provide

Table 1
Results of a case study to obtain the accuracy ratio for the Optech ILRIS 3D LIDAR system.

Scan resolution	Medium (5 mm)			Fine (3 mm)		
Target distance	7 m	15 m	30 m	7 m	15 m	30 m
Accuracy of target 1	3.2	3.0	4.0	2.7	3.0	4.2
Accuracy of target 2	4.1	4.8	5.2	3.3	3.4	4.5
Average accuracy	4.05			3.52		

3D coordinated surface data in a short time with high-precision measurements that are cost-effective, very mobile, easy to use, and maintainable. Moreover, considering that the accuracy of LIDAR measurements varies within a few millimetres, this system can be suitable for monitoring aseismic slip, which has a rate greater than this scale.

Using the Optech ILRIS 3D model for the LIDAR system, we scanned three manmade walls across the NAF during six field campaigns between July 2007 and December 2009. In order to provide consistent distances and aspect angles between the periodic studies, fixed stations placed into concrete at each location were used in the field measurements.

A LIDAR scan of an object produces a 3D point cloud (Fig. 2). The PolyWorks 10.0 software was used to process and clean all noise from the obtained point clouds in this study. The first measurement carried out in July 2007 at each site was assumed to be the base for the following measurements. After each campaign, new measurements were compared with both the first measurements (obtained in July 2007) and those of previous campaigns (see Supplementary Fig. S1 for a sample process).

3. Surface creep along the NAF

Aseismic surface creep on the NAF was first noticed by Ambraseys (1970) at the Ismetpasa section, which experienced surface faulting during the 1944 Bolu-Gerede (Ms = 7.3) earthquake (Fig. 1a). In the following 6 yrs, the fault at the same site apparently manifested aseismic surface slip of about 0.3 m before rupturing again during the 1951 earthquake (Ambraseys, 1970; Barka, 1996; Pinar, 1953; Saroglu et al., 1992). Between 1957 and 1999, the NAF experienced four major shocks on the western part of the Ismetpasa site (Fig. 1a), namely, at Abant (Ms = 7.0), Mudurnu (Ms = 7.1), Izmit (Ms = 7.4), and Duzce (Ms = 7.2). For the 1999 earthquakes, Dogan et al. (2002) proposed a right-lateral triggered slip of up to 6 cm around the railway station in Ismetpasa and Hamamlı Village (Fig. 3a) along the creeping section of the NAF, but no slip was reported for the 1957 Abant and 1967 Mudurnu earthquakes.

Using a tape metre, Ambraseys (1970) estimated a creep rate of 20 mm/yr. Following Ambraseys (1970), a small geodetic network of 6 points was established across the fault near the Hamamlı Village. Using this network, Aytun (1982), Deniz et al. (1993), and Kutoglu and Akcın (2006) estimated creep rates of 11 ± 1.1, 9.3 ± 0.7, and 7.8 ± 0.5 mm/yr, respectively. InSAR observations made by Cakir et al. (2005) provided a rate of about 8 ± 3 mm/yr between 1992 and 2001 and a length of 60–70 km for the creeping section at Ismetpasa. Although Dogan et al. (2002) claimed some triggered slip at the Ismetpasa railway station and Hamamlı Village sites after the 1999 earthquakes, GPS measurements by Kutoglu and Akcın (2006) and InSAR measurements by Cakir et al. (2005) and Cakir and Akoglu (2008) rule out any triggered slip after these events. Kutoglu et al. (2008) claimed a sudden increase in creep rate to 12 ± 1.1 mm/yr since 2002 and suggested that a creep may not be transient but varies with time (i.e. it is episodic). The recently estimated creep rate of 12 ± 1.1 mm/yr suggests an increase of more than 50%, but what caused this increase was not explained. There have been no moderate or large earthquakes since 2002 that may have given rise to the increase in the creep rate.

A second creeping section along the NAF was recently discovered on a wall across the rupture of the 26 November 1943 Tosya earthquake (Ms = 7.6) in Destek (Figs. 1a and b, and 3b). A stone wall was constructed across the 1943 Tosya rupture in 1980, and we noticed in 2003 that there is a warp towards the west in this wall (Fig. 4a). This wall collapsed in 2004, and a concrete wall was rebuilt at the same location (Fig. 4b). Warping of the wall with time and its collapse suggest a creep on the fault. The new wall has not cracked yet but tends to bend (Fig. 4b).

4. LIDAR campaigns

Two walls located across the 1944 Bolu-Gerede earthquake rupture (Fig. 2a) were scanned at 3-mm resolution during six campaigns at Ismetpasa. The first site in this section was the wall of the railway station reported by Ambraseys (1970) (Figs. 3a and 5a). The 20-m-long and 60-cm-high wall was constructed in 1957, obliquely across the fault, at an angle of 75°. Since then, the wall has warped, cracked, and offset by about 40 cm because of fault creep (Fig. 5a). The second site is located in the Hamamlı Village about 2 km east of the Ismetpasa railway station (Fig. 3a), where the geodetic network exists. It is a 10-m-long and 2.5-m-high cowshed wall built in 2000 (Fig. 5b). The wall and fault are nearly orthogonal (~80°) to each other. It is partially broken as a result of creeping (inset photograph in Fig. 5b). LIDAR measurements were conducted at a third site located in Destek along the NAF (Fig. 3b). A stone wall about 16 m long and 1.5 m high was scanned (Figs. 2b and 4b). The angle between the wall and fault is 80°.

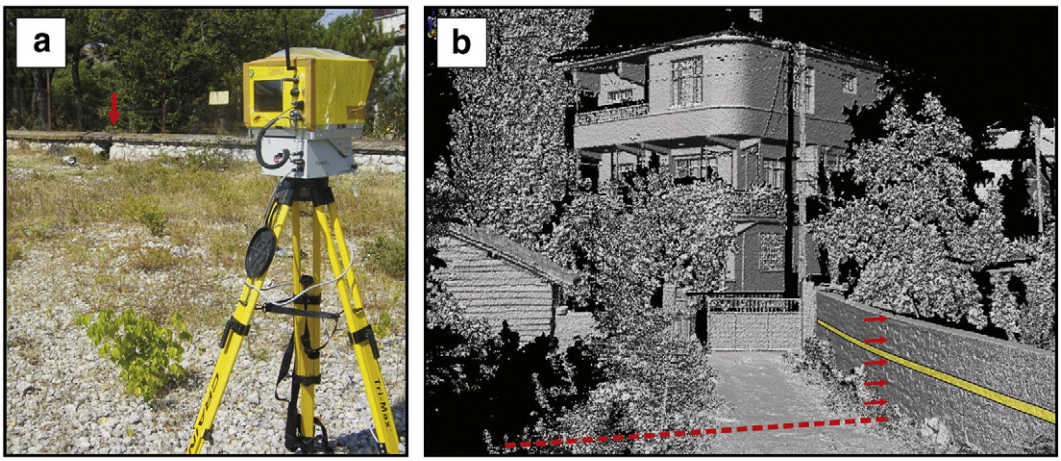

Fig. 2. (a) Optech ILRIS 3D LIDAR. The broken wall (red arrow) in the railway station near Ismetpasa is visible in the background. (b) 3D point cloud obtained with LIDAR. The wall in the bottom right corner was scanned in this study. The dashed red line is the trace of the fault; red arrows indicate the centre of the bending on the wall; the yellow horizontal band on the wall is the selected surface for the data process.

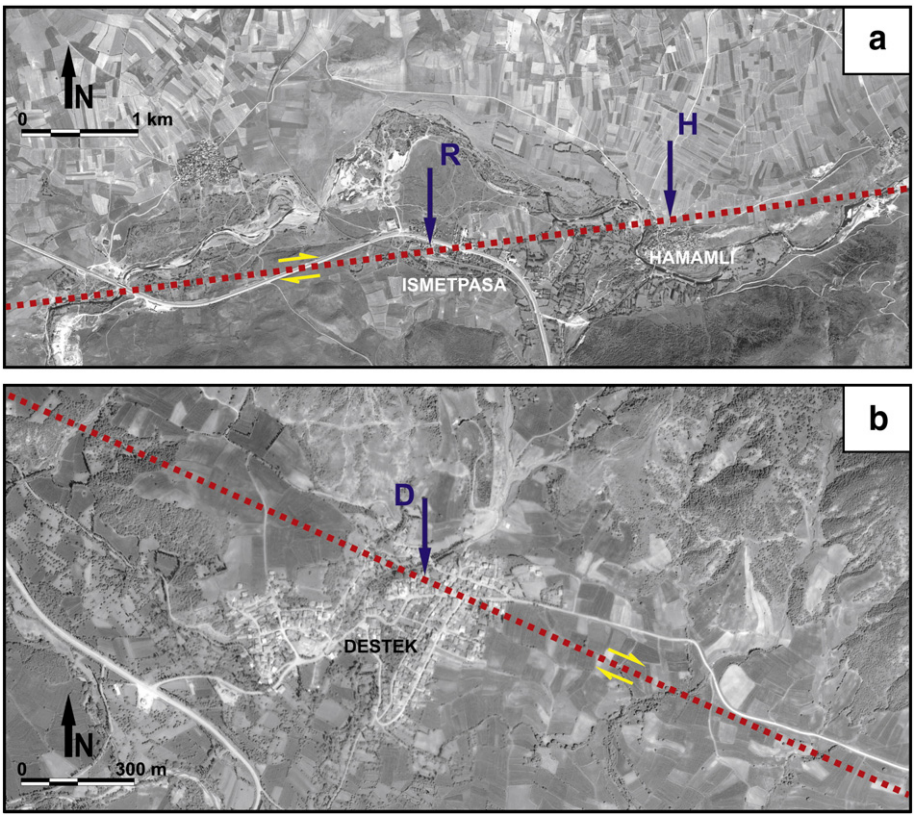

Fig. 3. (a) Detailed map of the Ismetpasa site showing locations of surveyed walls in Ismetpasa. "R" is the wall of the railway station, "H" is the cowshed wall in the Hamamlı Village, and the dashed line is the trace of the NAF. (b) Detailed map showing the location of the surveyed wall (D) in Destek. The dashed line is the trace of the NAF. Satellite images are from Google Earth software.

As mentioned above, the output of the collected data is a point cloud, which is processed using PolyWorks 10.0 software, which can analyse dense point clouds in both planar view and 3D. Point clouds of each campaign were compared with that of the first campaign (i.e. July 2007), which was assumed to be the base. In order to get a precise overlay of the planar surfaces, the point clouds were overlaid in 3D. Following this step, we selected a 5- to 10-cm-wide horizontal band on the scanned surface (Fig. 2b). Three criteria were used in selecting the band: (1) the band should represent the maximum length on the scanned surface, (2) be at the minimum height above the top level of the seasonal plants, where the laser may have been blocked by plants, and (3) be at the maximum distance from the top of the wall, as environmental effects are more likely to be seen near the top of the wall. We fixed the band representing the base data (i.e. July 2007) with the bands of subsequent campaigns on one side of the fault and measured the displacement on the other side in plane view (Fig. 6). Table 2 shows the cumulative displacements obtained from the data of the periodic LIDAR campaigns and lists the estimated slip rate for each location. The amount of cumulative displacement is found to increase with time (Table 2).

Fig. 4. (a) Close-up view of the wall in Destek before 2004. Note the outward bending of the wall. (b) Close-up view of the present wall scanned during this study at the Destek site (263150 E, 4526687 N, 37). Note the difference in the style of construction.

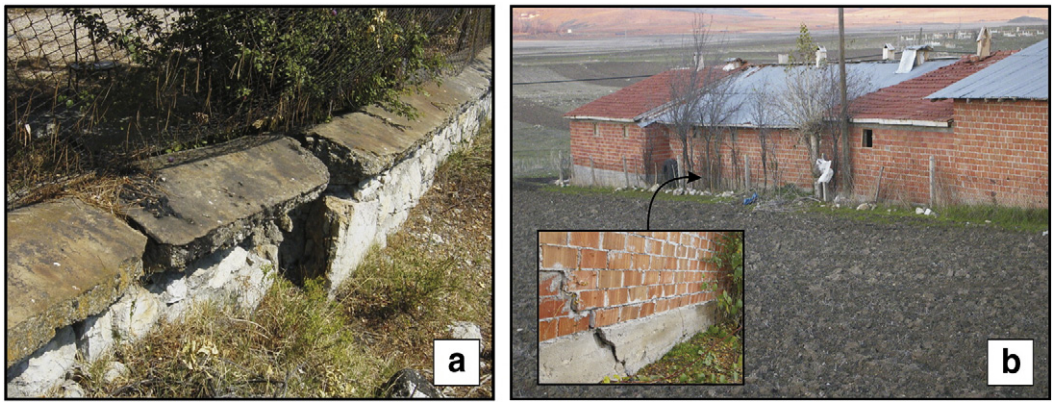

Fig. 5. (a) Close-up view of the creeping wall in the railway station in Ismetpasa (468453 E, 4524560 N, 36). (b) A general view of the scanned wall in Hamamlı Village (470350 E, 4524777 N, 36); the inset photograph is the close-up view of the broken part of the wall.

5. Discussion

Our surveys reveal that a significant amount of aseismic strain is being continuously released along the considered sections of the NAF:

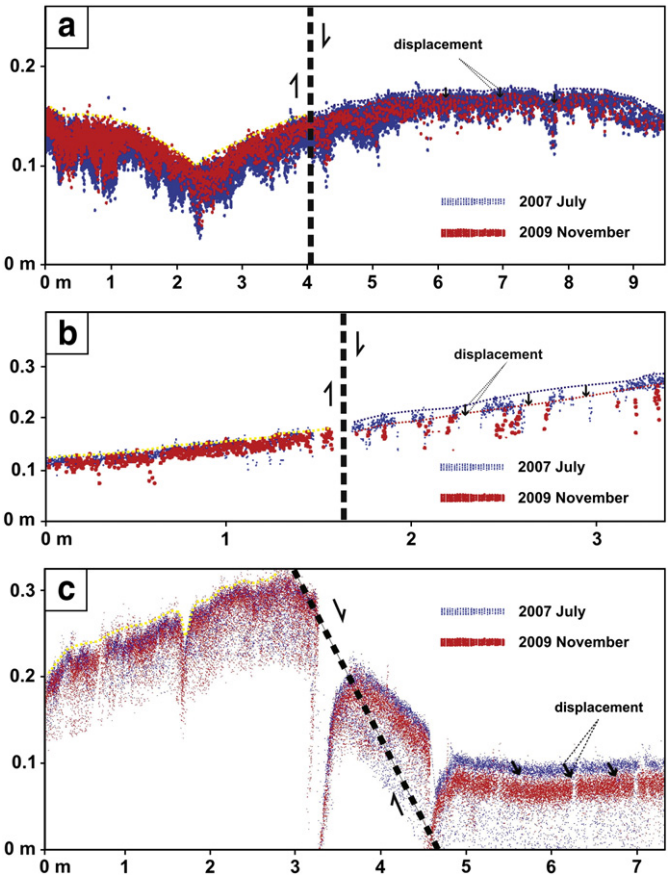

Fig. 6. Plane view of the point cloud obtained with LIDAR. The dashed black line is the fault. The blue point cloud represents the first measurement (July 2007), which was assumed as the base data. The red point cloud represents the last measurement (November 2009). Overlapping the base data (July 2007) with the last data (November 2009) in the left side of the fault showed a displacement (black arrows) on the other side of the fault. In order to help readers see this easily, the edges of the point clouds are marked with a blue dashed line for the July 2007 data and with a red dashed line for the November 2009 data. The distance between the blue and red lines is the amount of cumulative slip for 30 months. (a) Destek site, (b) Hamamlı site, (c) railway station site.

6.8–10.0 ± 4.0 mm/yr and 9.1–10.1 ± 4.0 mm/yr at two sites near Ismetpasa and 6.0–7.2 ± 4.0 mm/yr at Destek. Nevertheless, these fault segments can still lead to large earthquakes because 50–70% of the yearly slip (i.e. 20–25 mm/yr) still accumulates on the fault. The occurrence of the 1943, 1944, and 1951 earthquakes validates this assumption.

Fig. 7 compares the LIDAR results with previous studies across the 1944 Bolu-Gerede earthquake rupture. Our results for Ismetpasa are clearly less than those estimated by Ambraseys (1970). It would not be realistic to compare our results with his estimation for the following reasons: (1) he did not include an error bar and (2) Dogan et al. (2002) observed a triggered slip of about 6 cm near Ismetpasa after the 1999 earthquakes that may have increased our results. As Fig. 7 shows, our estimated creep rate is slightly larger than the results from studies using other instrumental methods and models (Altay and Sav, 1991; Aytun, 1982; Cakir et al., 2005; Deniz et al., 1993; Kutoglu and Akcın, 2006) but smaller than the results of Kutoglu et al. (2008). It is worth noting that except for Kutoglu et al. (2008) and this study, all other studies were begun before the 1999 Izmit and Duzce earthquakes (Fig. 7). In addition, as mentioned above, Dogan et al. (2002) observed a triggered slip at the Ismetpasa railway station and Hamamlı Village sites after the 1999 earthquakes. Thus, there are two plausible interpretations: (1) The slightly larger aseismic slip rate obtained in this study may be because of the 1999 major shocks further west of Ismetpasa, as suggested by Sylvester (2004) and Lee et al. (2005), so the long term rate of creep may vary before or after earthquakes. If this is the case, it may now be decreasing exponentially to its pre-earthquake rate. (2) If the creep was not increased as a result of the 1999 events, it may now match its pre-earthquake rate, which seems likely since the creep rate appeared to be stable over the last 15 yrs with no clear sign of any effect of recent large earthquakes nearby (Fig. 7). Thus, these creeping sections should be continuously monitored to better understand their natures.

To our knowledge, there are no published data of creeping at the Destek site, where we estimated a creep rate of 6.0–7.2 ± 4.0 mm/yr; this is about 30–40% of the geomorphologically (Kozacı et al., 2007) and geodetically (Reilinger et al., 2006) estimated slip rate. Fraser et al. (2009) performed a paleoseismic trench study about 10 km west of the Destek site (Fig. 1b) and identified 7 earthquakes in the last 2.7 ka, where Barka (1996) reported 2.3 m of coseismic offset during the 1943 event. Assuming a characteristic earthquake slip of 2.3 m, Fraser et al. (2009) estimated a slip rate of 6 mm/yr for this part of the NAF and suggested a considerable amount of slip deficit for this segment. However, it seems unrealistic to assume that this section of the NAF may exhibit characteristic earthquake behaviour without tight constraints on the recurrence interval of the earthquakes and

Table 2
Amount of cumulative displacements and estimated aseismic slip rate for each site.

Location	Point cloud band		Cumulative displacement (mm)				Statistical analyses		
	Height (cm)	Width (cm)	July 2007	December 2008	July 2009	November 2009	Calculated slip (mm/yr)	Standard error of mean	R^2
Railway station, Ismetpasa	30	7	0	15	n.a.	19	8.4	±1.6	0.96
Hamamlı Village, Ismetpasa	150	10	0	n.a.	20	22	9.6	±0.5	0.99
Destek Village	70	5	0	10	12	16	6.6	±0.6	0.98

n.a.: not applicable.

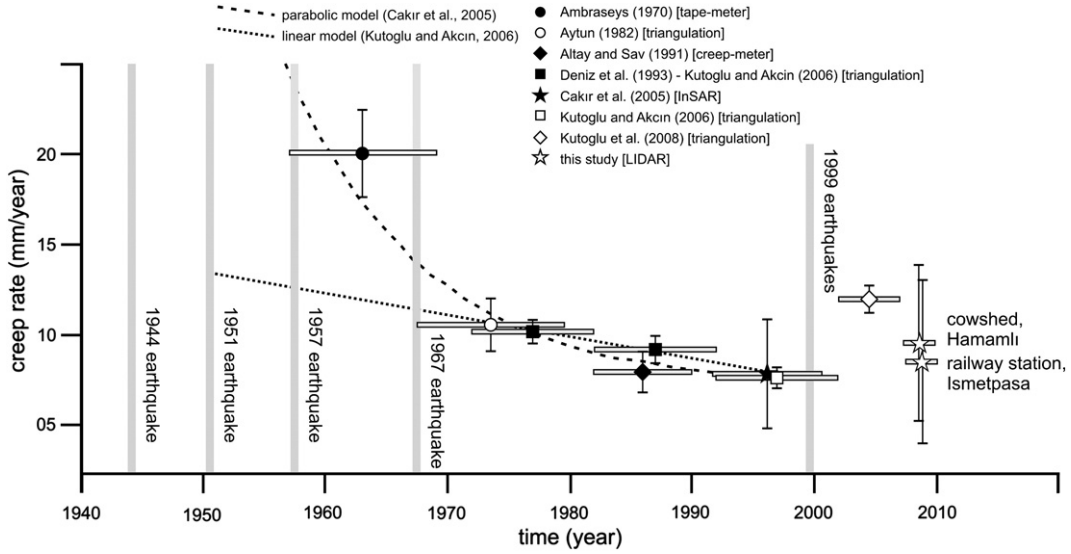

Fig. 7. Aseismic slip rates obtained from various studies near Ismetpasa (adapted from Cakir et al., 2005; Kutoglu and Akcın, 2006). Horizontal bars represent the monitoring time window. Vertical bars show the error ranges.

total cumulative slip they cause, especially when considering that a 6 mm/yr slip rate corresponds to only about 30% of the geodetically and geomorphologically estimated slip rates (Kozacı et al., 2007; Reilinger et al., 2006). The lateral extent of the surface creep is not known. If it continues westward and reaches the trench site, the slip deficit can be attributed to an aseismic surface creep, as in the case of characteristic earthquake models.

6. Conclusions

In this study, we demonstrated that LIDAR technology can be successfully applied to determine surface creep with its high resolution and accurate 3D measurement capability in very short times. Aseismic slip on the NAF was monitored between June 2007 and November 2009 by using a ground-based LIDAR system. The LIDAR system provided creep rates of 6.8–10.0 ± 4.0 and 9.1–10.1 ± 4.0 mm/yr at two sites near Ismetpasa. Comparing our creep rates with previous results showed that an aseismic slip is going on near Ismetpasa.

Another aseismic surface slip phenomenon along the NAF was recognised in Destek, which was not reported before. LIDAR results on this part of the fault showed an aseismic slip rate of 6.0–7.2 ± 4.0 mm/yr, which releases considerable amount of strain in this part of the NAF. Estimated creep rates using LIDAR were less than the geomorphic and geodetic slip rates (20–25 mm/yr) at both the Ismetpasa and Destek sites. However, these sections of the NAF are still capable of generating large earthquakes since 50–70% of the yearly slip still accumulates on the fault. The well-known 20th century earthquake sequence of 1939–1999 validates this assumption.

Supplementary data associated with this article can be found, in the online version, at doi:10.1016/j.epsl.2011.01.017.

Acknowledgement

This research was supported by the Eskisehir Osmangazi University Research Foundation (200615006 and 200615026). The authors are grateful to Mr. Önder Yönlü for his assistance in the field. Thanks go to R. Bengü Karabacak for her help on statistical computations. The authors are grateful for the helpful comments and constructive reviews by three anonymous reviewers which improved the manuscript.

References

Altay, C., Sav, H., 1991. Continuous creep measurement along the North Anatolian Fault zone. Turk. Jeol. Kuru. Bul. 6, 77–84.
Ambraseys, N.N., 1970. Some characteristic features of the Anatolian fault zone. Tectonophysics 9, 143–165.
Aytun, A., 1982. Creep measurements in the Ismetpasa region of the North Anatolian Fault zone. In: Isikara, A.M., Vogel, A. (Eds.), Proceedings, Multidisplinary Approach to Earthquake Prediction. Friedr. Vieweg and Sohn, Braunshweig/Wiesbaden, pp. 279–292.
Barka, A.A., 1996. Slip distribution along the North Anatolian fault associated with the large earthquakes of the period 1939 to 1967. Bull. Seismol. Soc. Am. 86 (5), 1238–1254.
Bawden, G.W., Kayen, R., Silver, M.H., Brandt, J.T., Collins, B.D., 2004. Evaluating tripod Lidar as an earthquake response tool. EOS Trans. Am. Geophys. Union 85 Fall Meet. Suppl. Abstract.
Bellian, J.A., Kerans, C., Jennette, D.C., 2005. Digital outcrop models: applications of terrestrial scanning lidar technology in stratigraphic modeling. J. Sed. Res. 75, 166–176.
Bonnaffe, F., Jennette, D., Andrews, J., 2007. A method for acquiring and processing ground-based lidar data in difficult to access outcrops for use in three dimensional, virtual reality models. Geosphere 3 (6), 501–510.

Burtford, R.O., Harsh, P.W., 1980. Slip on the San Andreas fault in central California from alignment array surveys. Bull. Seismol. Soc. Am. 70, 1223–1261.
Cakir, Z., Akoglu, A.M., 2008. Synthetic aperture radar interferometry observations of the M = 6.0 Orta earthquake of 6 June 2000 (NW Turkey): reactivation of a listric fault. Geochem. Geophys. Geosyst. 9. doi:10.1029/2008GC002031 Q08009.
Cakir, Z., Akoglu, A.M., Belabbes, S., Ergintav, S., Meghraoui, M., 2005. Creeping along the Ismetpasa section of the North Anatolian fault (Western Turkey): rate and extent from InSAR. Earth Planet. Sci. Lett. 238, 225–234.
Deniz, R., Aksoy, A., Yalın, D., Seeger, H., Franke, P., Hirsch, O., Bautsch, P., 1993. Determination of crustal movements in Turkey by terrestrial geodetic methods. J. Geodyn. 18, 13–22.
Dogan, A., Kondo, H., Emre, O., Awata, Y., Ozalp, S., Tokay, E., Yildirim, C., 2002. Stable creeping and distant triggered slips by the 1999 Izmit Earthquake along the Ismetpasa section, North Anatolian fault zone, Turkey. Eos, Trans.—Am. Geophys. Union 83 (47) Fall Meet. Suppl. Abstract, S11B-1156.
Ekercin, S., Üstün, B., 2004. A new technology in remote sensing: LIDAR. J. Geod. Geoinf. 91, 34–38.
Fraser, J., Pigati, J.S., Hubert-Ferrari, A., Vanneste, K., Avsar, U., Altınok, S., 2009. A 3000-year record of ground-rupturing earthquakes along the central North Anatolian Fault near Lake Ladik, Turkey. Bull. Seismol. Soc. Am. 99 (5), 2681–2703.
Hubert-Ferrari, A., Armijo, R., King, G., Meyer, B., Barka, A., 2002. Morphology, displacement and slip rates along the North Anatolian Fault Turkey. J. Geophys. Res. 107, 22–35.
Janson, X., Kerans, C., Bellian, J.A., Fitchen, W., 2007. Three dimensional geological and synthetic model of Early Permian redeposited basinal carbonate deposits, Victorio Canyon, West Texas. AAPG Bull. 91 (10), 1–32.
Kayen, R., 2004. Ground-based LIDAR. *GEER*, 10-07-2004 Meeting.
Kemeny, J., Turner, K., 2008. Ground-based LIDAR rock slope mapping and assessment. Federal Highway Administration Report, Lakewood, USA.
Kozacı, O., Dolan, J.F., Finkel, C.F., Hartleb, R., 2007. Late Holocene slip rate for the North Anatolian fault, Turkey, from cosmogenic 36Cl geochronology: Implications for the constancy of fault loading and strain release rates. Geology 35 (10), 867–870.
Kozacı, O., Dolan, J.F., Finkel, C.F., 2009. A late Holocene slip rate for the central North Anatolian fault, at Tahtakopru, Turkey, from cosmogenic 10BE geochronology: implications for fault loading and strain release rates. J. Geophys. Res. 114, B01405.
Kutoglu, H.S., Akcın, H., 2006. Determination of the 30-year creep trend on the Ismetpasa segment of the North Anatolian Fault using an old geodetic network. Earth Planet. Space 58 (8), 937–942.
Kutoglu, H.S., Akcın, H., Kemaldere, H., Görmüs, K.S., 2008. Triggered creep rate on the Ismetpasa segment of the North Anatolian Fault. Nat. Hazards Earth Syst. Sci. 8, 1369–1373.
Lee, J.C., Angelier, J., Chu, H.T., Hu, J.C., Jeng, F.S., 2005. Monitoring active fault creep as a tool in seismic hazard mitigation. Insights from creepmeter study at Chihshang, Taiwan. C. R. Geosci. 337, 1200–1207.
Lienkaemper, J.J., Williams, P.L., 1999. Evidence for surface rupture in 1868 on the Hayward fault in north Oakland and major rupturing in prehistoric earthquakes. Geophys. Res. Lett. 26, 1949–1952.
McClusky, S.C., Balassanian, S., Barka, A., Ergintav, S., Georgie, I., Gurkan, O., Hamburger, M., Hurst, K., Kahle, H., Kastens, K., Kekelidse, G., King, R., Kotzev, V., Lenk, O., Mahmout, S., Mishin, A., Nadaria, M., Ouzounis, A., Paradisissis, D., Peter, Y., Pirilepin, M., Reilinger, R.E., Sanli, I., Seeger, H., Teableb, A., Toksöz, N., Veis, V., 2000. Global positioning system constraints on plate kinematics and dynamics in the eastern Mediterranean Caucasus. J. Geophys. Res. 105, 5695–5719.
Nagihara, S., 2006. Use of Ground-Based LIDAR in Geomorphic and Surface Stratigraphic Studies. GCAGS/GCSSEPM, September 25–27, Lafayette.
Niemi, T.M., Kayen, R., Zhang, H., Dunn, C.R., Doolin, D.M., 2004. LIDAR imagery of the San Andreas Fault zone at the Vedanta and Olema Ridge paleoseismic trench sites, Pt. Reyes, CA. Eos, Trans.—Am. Geophys. Union Fall Meet. Suppl. Abstract.
Optech, 2006. The Basics: LIDAR, or Laser Radar. http://optech.ca/aboutlaser.htm.
Pinar, N., 1953. Etude ge'ologique et macrosismique du tremblement de terre de Kursunlu (Anatolie septentrionale) du 13 aout 1951. Rev. Fac. Sci. Univ. Istanbul A 18, 131–141.
POB, 2008. Point of Beginning, 2008 Laser Scanner Survey. http://laser.jadaproductions.net/.
Reilinger, R., McClusky, S., Vernant, P., Lawrence, S., Ergintav, S., Cakmak, R., Ozener, H., Kadirov, F., Guliev, I., Stepanyan, R., Nadariya, M., Hahubia, G., Mahmoud, S., Sakr, K., ArRajehi, A., Paradissis, D., Al-Aydrus, A., Prilepin, M., Guseva, T., Evren, E., Dmitrotsa, A., Filikov, S.V., Gomez, F., Al-Ghazzi, R., Karam, G., 2006. GPS constraints on continental deformation in the Africa–Arabia–Eurasia continental collision zone and implications for the dynamics of plate interactions. J. Geophys. Res. 111, 1–26.
Saroglu, F., Emre, O., Kuscu, I., 1992. Active Fault Map of Turkey. General Directorate of Mineral Research and Exploration, Ankara.
Schimdt, D.A., Bürgmann, R., Nadeau, R.M., d'Alessio, M.A., 2005. Distribution of aseismic slip-rate on the Hayward fault inferred from seismic and geodetic data. J. Geophys. Res. 110, B08406. doi:10.1029/2004JB003397.
Staiger, R., 2003. Terrestrial laser scanning technology, systems and applications. 2. FIG Regional Conference, December 2–5, Marrakech, Morocco.
Sylvester, A.G., 2004. Near-Field Tectonic Geodesy. http://books.nap.edu/books/0309036380/html/164.html#pagetop.
Thatcher, W., 1979. Systematic inversion of geodetic data in central California. J. Geophys. Res. 84, 2283–2297.